

## Impedance interaction between islanded parallel voltage source inverters and the distribution network

ISSA, Walid, ABUSARA, M A and SHARKH, S M

Available from Sheffield Hallam University Research Archive (SHURA) at:

<http://shura.shu.ac.uk/15264/>

---

This document is the author deposited version. You are advised to consult the publisher's version if you wish to cite from it.

### Published version

ISSA, Walid, ABUSARA, M A and SHARKH, S M (2014). Impedance interaction between islanded parallel voltage source inverters and the distribution network. In: Power Electronics, Machines and Drives (PEMD 2014), 7th IET International Conference on. IET.

---

### Repository use policy

Copyright © and Moral Rights for the papers on this site are retained by the individual authors and/or other copyright owners. Users may download and/or print one copy of any article(s) in SHURA to facilitate their private study or for non-commercial research. You may not engage in further distribution of the material or use it for any profit-making activities or any commercial gain.

# Impedance Interaction between Islanded Parallel Voltage Source Inverters and the Distribution Network

W. R. Issa\*, M. A. Abusara\*, and S. M. Sharkh<sup>†</sup>

\*Exeter University, UK (wrmi201@exeter.ac.uk), <sup>†</sup>Southampton University, UK

**Keywords:** Island mode, Resonance, Output impedance

## Abstract

In an islanded microgrid consisting of parallel-connected inverters, the interaction between an inverter's output impedance (dominated by the inverter's filter and voltage controller) and the impedance of the distribution network (dominated by the other paralleled inverters' output impedances and the interconnecting power cables) might lead to instability. This paper studies this phenomenon using root locus analysis. A controller based on the second derivative of the output capacitor voltage is proposed to enhance the stability of the system. Matlab simulation results are presented to confirm the validity of the theoretical analysis and the robustness of the proposed controller.

## 1. Introduction

Microgrids are defined as systems that have at least one distributed generation (DG) unit and associated loads, and can work in grid-connected mode as well as in island mode [1]. Due to its controllability, microgrids will become building block of future smart grids. This technology can offer improved service reliability, better economics and reduced dependency on the local utility.

When controlling a microgrid, it is important to ensure the stability of each unit as well as the microgrid as a whole under different loads and system conditions. In many practical scenarios, the DGs are located far away from each other and therefore they are connected to the network via cables with non-negligible impedance. This could cause the voltage controllers of DGs working in parallel to become unstable.

Power sharing between parallel-connected DGs can be achieved using the well-known droop control [2]-[7]. Much research has also been done to enhance droop control to improve the accuracy of the power sharing between DGs [8]-[10]. The concept of the virtual impedance has been widely used to overcome the problem of power coupling caused by high R/X ratio in low voltage distribution networks [11, 12]. It increases the inductive reactance of the inverter's output impedance without using additional physical inductors that would increase size and cost. Each inverter is normally controlled by a core controller that regulates the inverter's output voltage, and an outer droop controller that sets the amplitude and frequency references for the inner core controller. The core controller has much higher bandwidth and hence faster response than that of the outer droop controller and therefore the dynamic behavior of the inner core controller is normally neglected in the design and analysis of the droop controller. Consequently, the interaction between the core

voltage controller and the distribution network (consisting of cables, loads and other inverters) is often discarded. However, in practice, the DGs voltage controller can become unstable due to the interaction between the output impedance of each inverter and other inverters and cable impedances that can create parallel and/or series resonance. If the resonance frequency is within the bandwidth of the voltage controller an instability could occur. Thus, designing the inverter controller as a single isolated unit does not guarantee stability in all conditions.

Different types of controller including PI, repetitive, resonant, deadbeat and many other controllers have been used in grid-connected inverters. They usually utilize dual loop control to dampen output filter resonance [13]-[16]. However, the interaction between the inverter and the network is rarely considered or addressed when designing these controllers. In [17], the interaction between uninterruptible power supplies (UPS) was investigated. The study recommended reducing the voltage controller bandwidth by manipulating the voltage and current controllers' gain to keep the system stable. In [18], the controller bandwidth was reduced by using a feedforward loop. Ref [18] also concluded that a resistive virtual impedance has no effect on the system stability. However, the effect of an inductive virtual impedance was not addressed.

In this paper, the effect of the inductive virtual impedance as well as cables' length on the stability of parallel-connected inverters is studied. A controller based on the second derivative of the output capacitor voltage is proposed to enhance the stability of the system. The proposed controller ensures stability over a range of cable impedance and virtual impedance values.

## 2. System modelling

Fig. 1 shows an islanded microgrid consisting of two inverters and their LC filters, cables and load. The parameters of the system considered in this paper are listed in Table 1.

Fig. 2 shows a block diagram of one inverter and its basic controller. It consists of an outer feedback loop of the capacitor voltage  $V_o$  and an inner feedback loop of the capacitor current  $I_c$  with the latter employed to provide damping to the filter resonance. In addition to the dual feedback loops of  $I_c$  and  $V_o$ , a feedforward loop of the reference voltage is also implemented to minimise the steady state error. Furthermore, a virtual impedance loop is used to make the output impedance of the inverter more inductive and hence increase the decoupling between active and reactive power. Thus, the active power is predominantly dependent on the power angle and the reactive power is predominantly dependent on the output voltage.

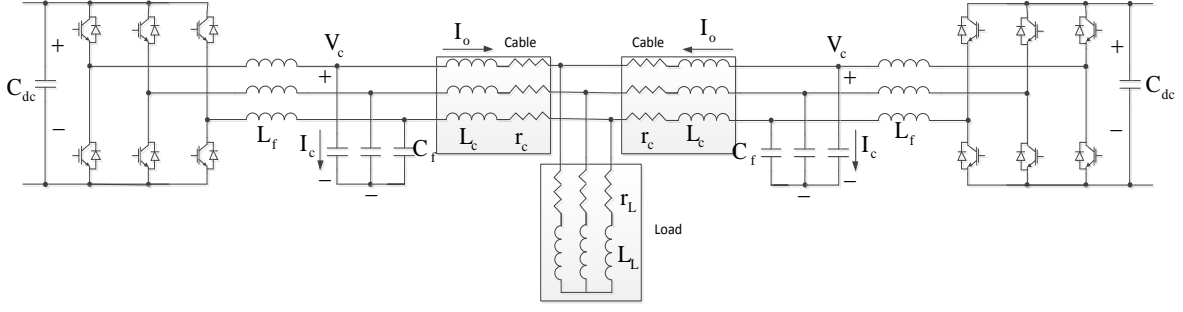


Fig. 1. Islanded Microgrid Structure

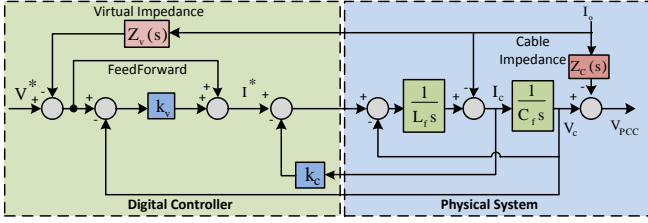


Fig. 2. The basic double-loop voltage controller of an inverter

Symbol	Description	Value
$L_f$	Inverter-side filter inductor	800 $\mu$ H
$C_f$	Filter capacitor	60 $\mu$ F
$k_v$	Voltage controller loop gain	2
$k_c$	Current controller loop gain	2.2
$r_c$	Cable resistance	$0.5 \times 10^{-3} \Omega / m$
$L_c$	Cable inductance	1 $\mu$ H / m
$L_v$	Nominal virtual inductance	650 $\mu$ H
$\tau$	Time constant (virtual impedance)	1/1500

Table 1. System Parameter Values

It can be shown from Fig. 2 that the output voltage is given by

$$V_o(s) = G(s)V^*(s) - Z_o(s)I_o(s) \quad (1)$$

where  $G(s)$  is the closed loop transfer function that relates  $V_o$  to  $V^*$  and  $Z(s)$  is the closed loop output impedance and they are given by

$$G(s) = \frac{k_v + 1}{L_f C_f s^2 + k_c C_f s + k_v + 1} \quad (2)$$

$$Z_o(s) = \frac{L_f s}{L_f C_f s^2 + k_c C_f s + 1 + k_v} + G(s)Z_v(s) \quad (3)$$

The virtual impedance transfer function  $Z_v(s)$  in (3) is given by

$$Z_v(s) = \frac{s}{\tau s + 1} L_v \quad (4)$$

where  $L_v$  is the inductance of the virtual impedance and  $\tau$  is the time constant of the high pass filter used to approximate the derivative in the transfer function of the ideal virtual inductance ( $Z_v = sL_v$ ). Fig. 3 shows the Thévenin equivalent circuit of a simple single inverter model represented by (1).

Fig. 4 shows the frequency response of the output impedance transfer function  $Z_o(s)$  with  $L_v$  equals to zero and 650 $\mu$ H. As can be seen, the output impedance has a predominant inductive behavior in the region below the natural frequency that is important for proper droop control operation, especially, around the fundamental frequency. There is a resonance at the natural frequency but it has been damped thanks to the inner current loop.

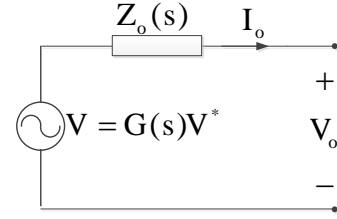


Fig. 3. Simple inverter model (Thévenin equivalent circuit)

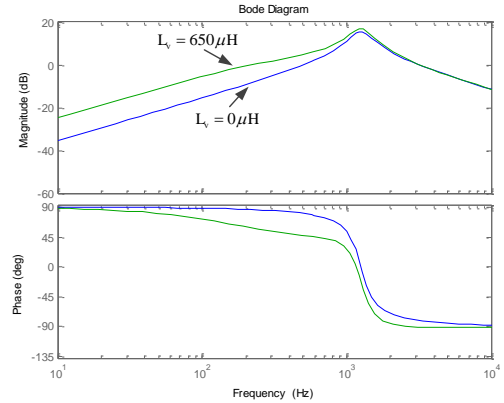


Fig. 4. Bode plot of output impedance with/without virtual impedance

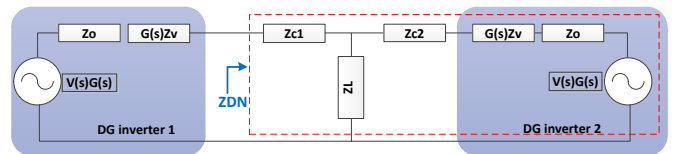


Fig. 5. General microgrid model

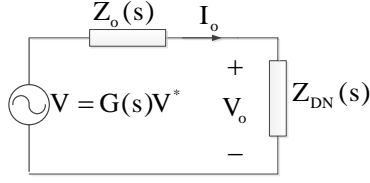


Fig. 6. Simplified Model

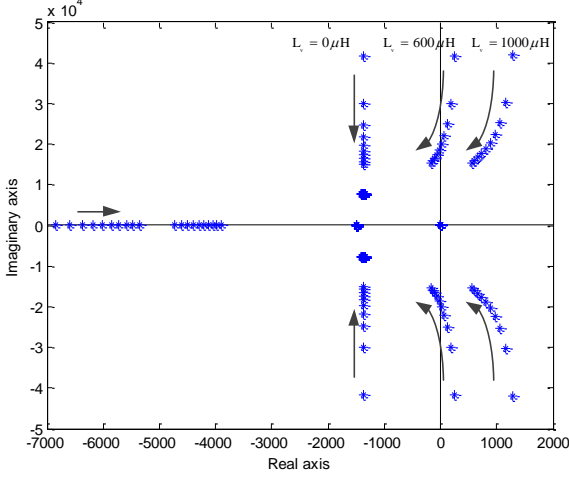


Fig. 7. Root locus when cable length varies from 10m to 100m, for value of  $L_v$  of 0, 600 and 1000 $\mu$ H

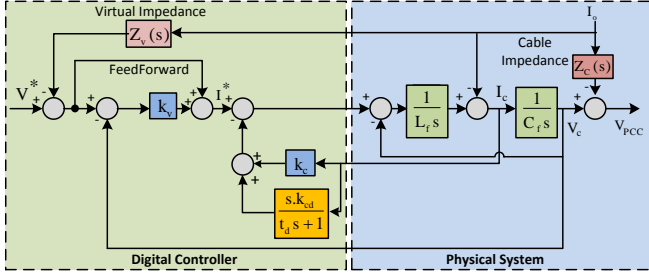


Fig. 8. The proposed voltage controller

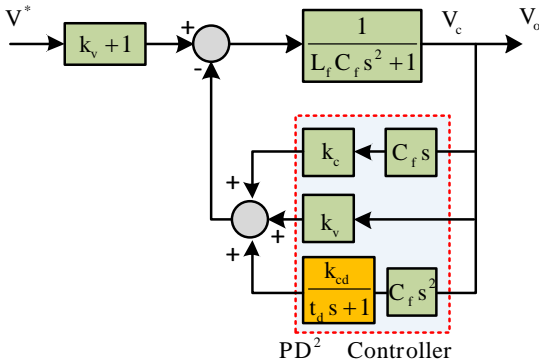


Fig. 9. The simplified proposed voltage controller loop

A circuit model for a microgrid consisting of two inverters connected through cables and supplying a common load is shown in

Fig. 5 where  $Z_{c1}$  and  $Z_{c2}$  are the impedances of the connecting cables. Using the superposition principle, i.e., by setting the voltage of the second inverter to zero, i.e.,  $G(s)V^*(s)=0$ , the

microgrid from the point of view of the first inverter can be modelled as shown in Fig. 6 where  $Z_{DN}(s)$  represents the equivalent impedance of the load, cables and the output impedance of the second inverter. The load impedance in this paper will be assumed very high (i.e., open circuit). This represents the worst-case scenario for resistive loads, as the load resistivity will increase the system damping. Therefore, the equivalent impedance  $Z_{DN}(s)$  is given by

$$Z_{DN}(s) = Z_{c1} + Z_{c2} + Z_o \quad (5)$$

From Fig. 6, the output voltage can be written as

$$V_o(s) = \frac{G(s)V_c^*(s) \times Z_{DN}(s)}{Z_o(s) + Z_{DN}(s)} \quad (6)$$

Equation (6) represents the closed loop transfer function relating the output voltage  $V_o$  to the reference voltage  $V^*$  taking into account the effect of the connecting cables and the impedance of the other inverters.

### 3. Stability Analysis

From (6), the root locus of the characteristics equation (7), can be used to analyze the system stability.

$$Z_o(s) + Z_{DN}(s) = 0 \quad (7)$$

The interaction between an inverter with the network containing cables and other inverters can be addressed using equation (7) in terms of the value of the virtual impedance and the length of cables.

The effect of the virtual impedance on stability is illustrated with the aids of the root locus as shown in Fig. 7. In this figure, the effect of cables length, change from 10m to 100m, on the closed loop poles of the system is shown for three virtual impedance values of 0, 600 and 1000 $\mu$ H; the arrows show the direction of increase of the cable length. As depicted, high values of virtual inductance (above 600 $\mu$ H) reduce the stability of the system. This can be explained to be due to the increase of the high frequency gain. The cable impedance also has a significant effect on the system. A combination of a short cable and a high virtual impedance value can destabilize the system. Increasing the length of the cable and hence its resistance improves system stability as expected.

### 4. Proposed controller

To improve the stability of the system we propose employing a feedback of the voltage second derivative to present more damping for the complex poles and shift them farther to the left. The new proposed controller is shown in Fig. 8.

As known, the capacitor current is given by the derivative of the voltage across it,

$$I_c = C_f \frac{dV_c}{dt} \quad (8)$$

The second derivative of voltage can be therefore used to obtain the derivative of the capacitor current as:

$$\frac{dI_c}{dt} = C_f \frac{d^2V_c}{dt^2} \quad (9)$$

Hence, the extra damping term could be realized by the first derivative of capacitor current, which presents a PD<sup>2</sup> controller instead of PD controller as shown in its simplified version in Fig. 9.

The PD<sup>2</sup> controller measures the change of rate of current change of rate that could reduce the disturbance effects on the system if proper gain is used to reject these disturbances.

The first derivative already can be measured directly by sensing the capacitor current. However, the second derivative needs to be calculated. Differentiation of the high-frequency capacitor current may cause serious noise multiplication problems that could lead to instability. Therefore, a low pass filter is added after the derivative term to minimize the effect of the high frequency on system stability. The full derivative followed by low pass filter is stated as:

$$s.I_c \cdot \frac{1}{\tau_d s + 1} \quad (10)$$

where  $\tau_d$  is the time constant of the filter.

The new version of the voltage closed loop transfer function is calculated as stated in (11), where  $k_{cd}$  is the derivative gain of the capacitor current.

The new output impedance is obtained from Fig. 8, with considering the virtual and cable impedances, as in equation (12).

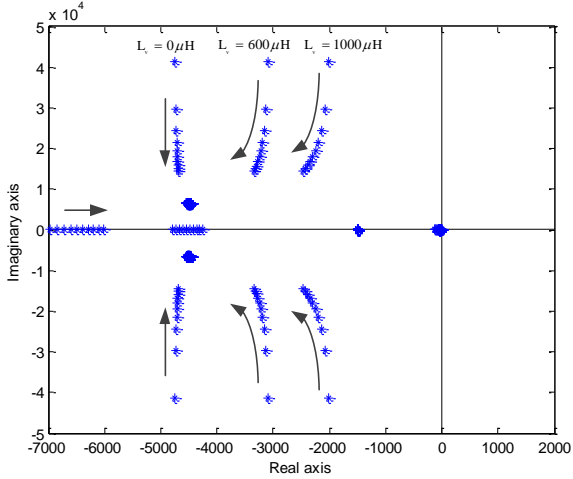


Fig. 10. Root locus with the proposed controller as the virtual inductance and cables length varies from 10-100 m

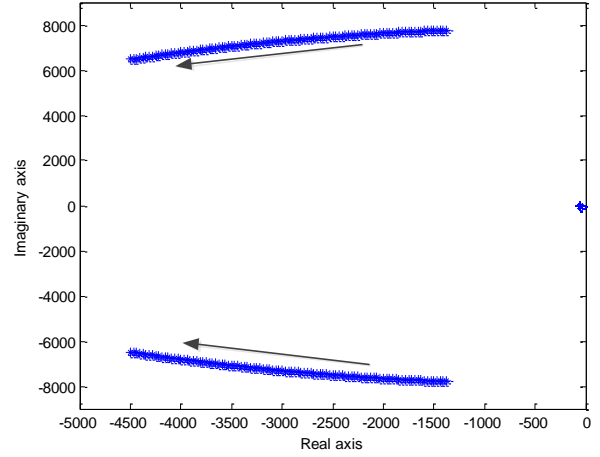


Fig. 11. Root locus of the voltage controller when  $k_{cd}$  varies from 0 to 0.1

Fig. 10 illustrates the effect of the proposed controller on stability. The root locus now shows that the system is stable for the range of virtual inductance values and cable lengths.

Fig. 11 illustrates the locus of  $G_p(s)$  when  $k_{cd}$  varies from 0 to 0.1 where  $\tau_d = 0.02$ . As shown, it shifts the oscillated components far away from the imaginary axis thus increasing stability.

## 5. Simulation results

Matlab model was built, as shown in Fig. 5, including two single-phase inverters modeled by two-leg IGBT bridge and voltage controller with capacitor voltage and current as feedback signals. They are connected via cables lengths 10m and 20m respectively. The model parameters are listed in Table 1. The voltages of the inverters are shown in Fig. 12 with and without the proposed controller. As shown, the system without the proposed controller is unstable as expected from the previous analysis while the stability is achieved with the proposed controller.

More results are obtained with the proposed controller shown in Fig. 13. The cable length of the second inverter has changed from 20m to 30m at  $t = 0.05$  sec concurrently with an increment step of the virtual inductance from 650 μH to 1000 μH. The results confirm the stability and illustrate the robustness of the proposed controller against different network and controller conditions.

$$G_p(s) = \frac{(k_v + 1)\tau_d s + k_v + 1}{L_f C_f \tau_d s^3 + (L_f C_f + C_f k_c \tau_d + C_f k_{cd})s^2 + (k_c C_f + \tau_d (k_v + 1))s + k_v + 1} \quad (11)$$

$$Z_{op}(s) = \frac{L_f \tau_d s^2 + L_f s}{L_f C_f \tau_d s^3 + (L_f C_f + C_f k_c \tau_d + C_f k_{cd})s^2 + (k_c C_f + \tau_d (k_v + 1))s + k_v + 1} + G_p(s)Z_v(s) + Z_c(s) \quad (12)$$

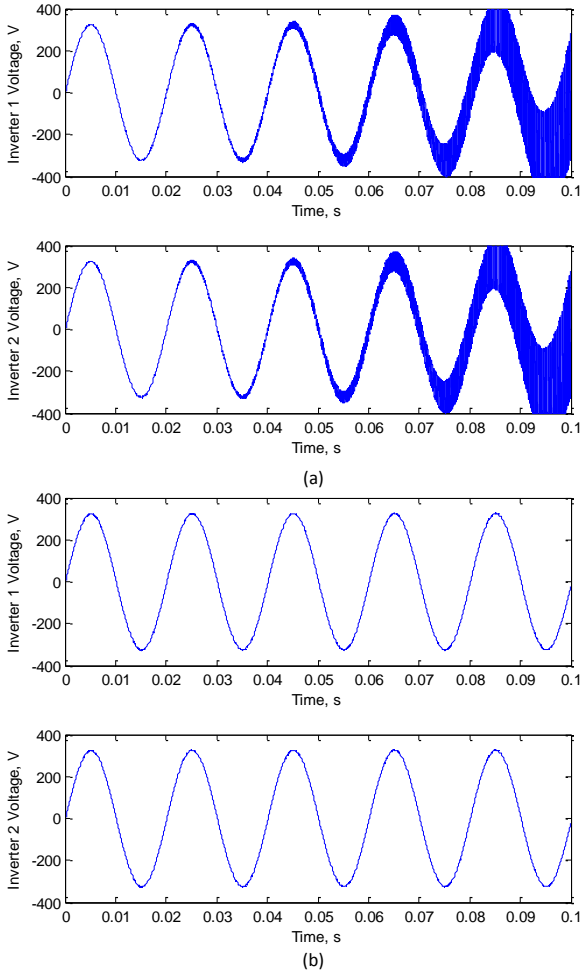


Fig. 12. Output voltages of the two inverters without (a) and with (b) the proposed control loop

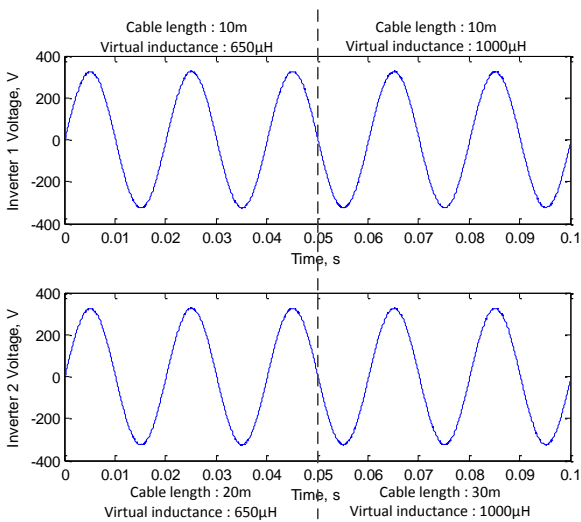


Fig. 13. Output voltages of the two inverters with the proposed control loop when the cable length and virtual inductance vary

## 6. Conclusion

This paper studies the interaction between the output impedance of microgrid inverters and the network impedance including interconnecting cables and the impedance of other parallel inverters. This interaction can destabilize the whole system. A novel controller that uses a feedback loop of the second derivative of the inverter's output voltage has been proposed to enhance stability. Matlab simulation results have verified the theoretical analysis and the validity of the proposed controller.

## References

- [1] B. Kroposki, R. Lasseter, T. Ise, S. Morozumi, S. Papatlianassiou, and N. Hatzargyriou, "Making microgrids work," *IEEE Power and Energy Magazine*, vol. 6, pp. 40-53, 2008.
- [2] B. B. K. Brabandere, J. Keybus, A. Woyte, J. Driesen, and R. Belmans, "A voltage and frequency droop control method for parallel inverters," *IEEE Trans. Ind. Electron.*, vol. 22, pp. 1107-1115, 2007.
- [3] J. C. Vasquez, J. M. Guerrero, A. Luna, P. Rodríguez, and R. Teodorescu, "Adaptive droop control applied to voltage-source inverters operating in grid-connected and islanded modes," *IEEE Transactions on Industrial Electronics*, vol. 56, pp. 4088-4096, 2009.
- [4] H. J. Avelar, W. A. Parreira, J. B. Vieira, L. C. G. de Freitas, and E. A. A. Coelho, "A State Equation Model of a Single-Phase Grid-Connected Inverter Using a Droop Control Scheme With Extra Phase Shift Control Action," *IEEE Transactions on Industrial Electronics*, vol. 59, pp. 1527-1537, 2012.
- [5] F. Luo, Y. Lai, C. K. Tse, and K. Loo, "A triple-droop control scheme for inverter-based microgrids," in *IECON 2012-38th IEEE Annual Conference on Industrial Electronics Society*, 2012, pp. 3368-3375.
- [6] M. Abusara and S. Sharkh, "Control of line interactive UPS systems in a Microgrid," in *IEEE International Symposium on Industrial Electronics (ISIE)*, 2011, pp. 1433-1440.
- [7] J. M. Guerrero, J. C. Vasquez, J. Matas, M. Castilla, and L. G. de Vicuna, "Control strategy for flexible microgrid based on parallel line-interactive UPS systems," *IEEE Transactions on Industrial Electronics*, vol. 56, pp. 726-736, 2009.
- [8] J. M. Guerrero, L. G. De Vicuna, J. Matas, M. Castilla, and J. Miret, "A wireless controller to enhance dynamic performance of parallel inverters in distributed generation systems," *IEEE Transactions on Power Electronics*, vol. 19, pp. 1205-1213, 2004.
- [9] H. Z. Xiaotian Zhang, Josep M. Guerrero, Xikui Ma, "Reactive Power Compensation for Parallel Inverters without Control Interconnections in Microgrid," *IECON 2008. 34th Annual Conference of IEEE Industrial Electronics*, 2008.

- [10] M. C. Wei Yao, José Matas, Josep M. Guerrero, Zhao-Ming Qian, "Design and Analysis of the Droop Control Method for Parallel Inverters Considering the Impact of the Complex Impedance on the Power Sharing," *IEEE Transactions on Industrial Electronics*, vol. 58, 2011.
- [11] M. Abusara, J. M. Guerrero, and S. Sharkh, "Line Interactive UPS for Microgrids," *IEEE Transactions on Industrial Electronics*, pp. 1-8, 2013.
- [12] J. Kim, J. M. Guerrero, P. Rodriguez, R. Teodorescu, and K. Nam, "Mode Adaptive Droop Control With Virtual Output Impedances for an Inverter-Based Flexible AC Microgrid," *IEEE Transactions on Power Electronics*, vol. 26, pp. 689-701, 2011.
- [13] R. Ortega, E. Figueres, G. Garcerá, C. L. Trujillo, and D. Velasco, "Control techniques for reduction of the total harmonic distortion in voltage applied to a single-phase inverter with nonlinear loads: Review," *Renewable and Sustainable Energy Reviews*, vol. 16, pp. 1754-1761, 2012.
- [14] M. A. Abusara, M. Jamil, and S. M. Sharkh, "Repetitive current control of an interleaved grid-connected inverter," in *IEEE International Symposium on Power Electronics for Distributed Generation Systems (PEDG)*, 2012 3rd, 2012, pp. 558-563.
- [15] G. Escobar, P. Mattavelli, A. M. Stankovic, A. A. Valdez, and J. Leyva-Ramos, "An adaptive control for UPS to compensate unbalance and harmonic distortion using a combined capacitor/load current sensing," *IEEE Transactions on Industrial Electronics* vol. 54, pp. 839-847, 2007.
- [16] P. Mattavelli, "An improved deadbeat control for UPS using disturbance observers," *IEEE Transactions on Industrial Electronics*, vol. 52, pp. 206-212, 2005.
- [17] L. Corradini, P. Mattavelli, M. Corradin, and F. Polo, "Analysis of Parallel Operation of Uninterruptible Power Supplies Loaded through Long Wiring Cables," in *Twenty-Fourth Annual IEEE Applied Power Electronics Conference and Exposition*, 2009, pp. 1276-1282.
- [18] X. Wang, F. Blaabjerg, Z. Chen, and W. Wu, "Resonance analysis in parallel voltage-controlled Distributed Generation inverters," in *Twenty-Eighth Annual IEEE Applied Power Electronics Conference and Exposition (APEC)*, 2013, pp. 2977-2983.